Laboratory and Field Studies of the Acoustics of Multiphase Ocean Bottom Materials

Preston S. Wilson
Applied Research Laboratories
The University of Texas at Austin
P.O. Box 8029
Austin, TX 78713-8029

phone: (512) 475-9093   fax: (512) 471-8727   email: pswilson@mail.utexas.edu

http://www.arlut.utexas.edu/
http://www.me.utexas.edu/~pswilson

LONG-TERM GOALS

The long-term scientific objective of this project is to increase our understanding of sound propagation in ocean bottom sediments, including water-saturated sands and muds, gas-bearing sands and muds, and sediments which support seagrass. This in turn benefits buried object detection, sonar operation and acoustic communications and mine detection in shallow water. This project also includes continued analysis of data collected during Shallow Water 06 (SW06), and development of apparatus and procedures, and planning for the Sediment Characterization Experiment 2015 (referred to herein as SCE15) and its 2014 pilot survey. Finally, continued laboratory studies of the acoustics of the multiphase sediment materials mentioned above are long-term goals, coupled with the development of techniques and apparatus for *in situ* acoustic classification of ocean bottoms and mine hunting for Naval fleet operations.

OBJECTIVES/APPROACH

The origin of this project was an Entry Level Faculty Award in 2005, then a follow-on grant for 2008–2009. In this time, impedance tube and resonator methods, originally developed by the author for the investigation of bubbly liquids [1, 2], have been successfully modified for the investigation of ocean bottom sediments [3, 4]. In addition, the technique has been applied to the study of gassy sediments [5, 6] and seagrasses [7, 8]. In Refs. [3] through [8], sound speeds have been measured from 100 Hz up to 300 kHz. This work resulted in the author being awarded the 2007 A.B. Wood medal in underwater acoustics [9]. Analysis of SW06 data has also resulted in sound speed and attenuation inferences down to 40 Hz [10]. We now continue the use of these experimental methods to investigate, control and exploit sound propagation in multiphase

1. REPORT DATE **2012**	2. REPORT TYPE **N/A**	3. DATES COVERED **-**	
4. TITLE AND SUBTITLE **Laboratory and Field Studies of the Acoustics of Multiphase Ocean Bottom Materials**		5a. CONTRACT NUMBER	
		5b. GRANT NUMBER	
		5c. PROGRAM ELEMENT NUMBER	
6. AUTHOR(S)		5d. PROJECT NUMBER	
		5e. TASK NUMBER	
		5f. WORK UNIT NUMBER	
7. PERFORMING ORGANIZATION NAME(S) AND ADDRESS(ES) **Applied Research Laboratory The Pennsylvania State University P.O. Box 30, MS3510D State College, PA 16804**		8. PERFORMING ORGANIZATION REPORT NUMBER	
9. SPONSORING/MONITORING AGENCY NAME(S) AND ADDRESS(ES)		10. SPONSOR/MONITOR'S ACRONYM(S)	
		11. SPONSOR/MONITOR'S REPORT NUMBER(S)	
12. DISTRIBUTION/AVAILABILITY STATEMENT **Approved for public release, distribution unlimited**			
13. SUPPLEMENTARY NOTES **The original document contains color images.**			
14. ABSTRACT			
15. SUBJECT TERMS			

16. SECURITY CLASSIFICATION OF:			17. LIMITATION OF ABSTRACT **SAR**	18. NUMBER OF PAGES **19**	19a. NAME OF RESPONSIBLE PERSON
a. REPORT **unclassified**	b. ABSTRACT **unclassified**	c. THIS PAGE **unclassified**			

ocean bottom sediments and shallow water environments. The five primary objectives are:

1) Continue our laboratory and field investigations of various artificial and natural multiphase ocean bottom materials using the tube and resonator-based laboratory techniques mentioned above as well as traditional time-of-flight techniques. The objective is to obtain sound speed and attenuation measurements with sufficient knowledge of the measurement uncertainty to facilitate meaningful model comparison on a wider range of sediment types and physical input parameters than we have been able to achieve thus far. We also completed both lab and field studies of attenuation in seagrass beds as a function of photosynthetic activity (which effects the seagrass's acoustic properties). Operationally from a naval mine hunting point-of-view, this also correlates to time of day and season of the year, as seagrass gas production goes dormant in the night in summer months and stays dormant throughout the winter months.

2) We continue to analyze data from SW06, and to make preparations for participation in future sea tests. The PI is co-supervisor of Jason Sagers, one of the recipients of the Special Awards in Ocean Acoustics Graduate Fellowships, who has been studying the predictability of acoustic intensity fluctuations induced by nonlinear internal waves during SW06. This part of the effort also included continued development of the combustive sound source (CSS) for towable water column deployment (impulsive shots for propagation measurements), and ocean bottom deployment (to provide a means to infer shear properties through inversion of geophone measurements as described in Refs. [11, 12]).

3) The PI is serving as co-chief scientist for an upcoming shallow water sea test, namely the Sediment Characterization Experiment scheduled to go to sea in the spring of 2015 including a pilot survey in the spring of 2014. The objective of this work for the reporting year was planning and preparation, in coordination with the current ONR sea test on reverberation and the upcoming sea test on on shelf/slope effects.

4) We continued development of an acoustic inversion technique to determine the 3-D sound speed distribution in parcels of ocean. The goal of this acoustic remote sensing technique is to provide increased knowledge of the ocean waveguide sound speed distribution for forward propagation models and also to provide input parameters to large-scale numerical ocean dynamics models. The technique greatly extends the footprint of CTD-based or thermistor-chain-based temperature surveys.

5) We developed a laboratory proof-of-concept bubble discriminating sonar demonstration that exploits several basic acoustical phenomena associated with air bubbles in water. This sonar system in envisioned to find mines in difficult shallow water environments containing significant concentrations of air bubbles, such as the surf zone and in seagrass meadows. The discrimination system is based on up to three characteristic markers that identify bubbles rather than solid objects such as mines. First, we induce a Doppler shift in the echo from bubbles alone, not from solid objects, by applying a high-amplitude acoustic excitation to the search area. The high amplitude sound causes the bubbles to move but not the solid objects, hence there is a Doppler shift.

If this is shift is detected at the appropriate time after the outgoing excitation pulse, then this indicates the target is a bubble. Doppler from background motion of the target is excluded because such Doppler returns would not be phase locked with the excitation pulse. The excitation pulse also causes nonlinear oscillation of the bubble, which results in echo harmonics, subharmonics and potentially intermodulation distortion. A more solid target is not excited into nonlinear motion by the incident pulse and hence does not return any harmonics or intermodulation distortion.

Personnel for this project: Preston S. Wilson serves as PI and is an Associate Professor in the Mechanical Engineering Department at the University of Texas at Austin (UTME), and is also an Associate Research Professor at the University's Applied Research Laboratories (ARL:UT). In addition to oversight, Wilson contributes significantly to many tasks, including modeling, instrument and experiment design, construction and operation. Kevin T. Hinojosa, a UT Aerospace Engineering senior and an Undergraduate Research Assistant on the project, serves as an electromechanical technician and provides machine shop, procurement, software and experimental support. Laura M. Tseng, a UT Physics junior also serves as an undergraduate research assistant with similar duties. Theodore F. Argo IV was a UTME PhD student who contributed to all aspects of the project and received his PhD in May 2012. Christopher J. Wilson was a UT Marine Science PhD student, who worked on the seagrass acoustics portion of this project. Chris was primarily funded by a fellowship he held independently, but he contributed to this effort, and received his PhD in December 2011. Jason D. Sagers was funded by an ONR graduate fellowship and conducted analysis of SW06 data. Jason was a UTME PhD student and finished his PhD in August 2012. Christopher Bender is funded on an ARL IR&D and works on the inversion technique, co-supervised by Megan Ballard. Kevin M. Lee works on the mine hunting sonar project with additional support provided by ARL:UT IR&D.

WORK COMPLETED and RESULTS

Objective 1—Laboratory sediment and multiphase ocean bottom materials investigation: *Water-saturated granular sediments:* The goal of this work was to extend the parameter range of laboratory experimental data on sound propagation in water-saturated sediments in order to exercise existing propagation models and to verify which model or which parts of models are correct. Grad student Argo completed a very extensive set of measurements and model comparisons, which were published in his dissertation [18]. Some examples of the work are shown. Figs. 1 and 2 show a collection of all of his sound speed and attenuation data in comparison to a wide array of similar measurements that have been reported in the literature. [19] Fig. 3 shows a single set of measurements in coarse/medium water-saturated sand over a wide frequency range. It was found that the BICSQS model [20] can be fit to either the sound speed or the attenuation (using different input parameters), and is a better fit than the Biot-Stoll model, [21] but neither model can be made to fit both sound speed and attenuation for the same set of input parameters. This is the most general conclusion that can be drawn from Argo's dissertation. In none of the many cases studied could any model correctly predict both sound speed and attenuation for a fixed set of input parameters.

Propagation through seagrass: A high-frequency (100 kHz) outdoor tank experiment was conducted in which attenuation through a model seagrass bed was studied as a function of circadian light intensity. Three Texas Gulf Coast species were studied, *Syringodium filiforme*, *Halodule wrightii*, and *Thalassia testudinum*. As expected, attenuation is related to light intensity and photosynthetic activity (because gas is produced during photosynthesis) but not the same way for all species. Three photosynthesis- and acoustics-related processes occur. The leaves of the seagrass plants become pressurized with photosynthetically-produced gas (hence, the leaf acoustic compliance is changed), bubbles form on the leaves, and when sufficiently large, the bubbles break off the leaves and enter into the water column. The mean acoustic intensity of energy transmitted throughout the seagrass canopy varied by 3.5 dB for *S. filiforme*, 4.4 dB for *T. testudinum* and 4.7 dB for *H. wrightii* over a 24-h period, with peak attenuation usually occurring in the early morning after the onset of the day's photosynthetic activity, and minimum attenuation occurring sometime at night, but the details of this behavior varied among the species, and the trend was not as strong for *T. testudinum*. Independent measurements of seagrass leaf tissue compressibility were also conducted using the resonator technique, and it was found that the changing acoustic compressibility of the leaf tissue (in addition to the presence of air bubbles in the water column) must play a role. In general, leaf tissue compressibility is decreased during light hours, but it is the combination of leaf tissue compressibility, the presence of free gas on the leaves and in the water column that regulate the overall acoustic loss. Since it was found that bubble size produced by each species was different, the acoustic frequency plays a role as well. These effects are shown in Fig. 4 where relative 100 kHz acoustic received level is shown as a function of time-of-day, along with solar photosynthetically active Radiation (PAR), which is a measure of the photosynthetically-important photon flux density. *S. filiforme* (Fig. 4a) shows peak attenuation (larger negative dB values on the vertical axis) between 8 am and 10 am, while *H. wrightii* shows peak attenuation from 2 am to 8 am. *T. testudinum* also shows the highest attenuation in the early morning but its trends were not as strong as the other two species. The point is, for a particular species, there is likely a best time of day to conduct mine hunting due to the diurnal attenuation cycle observed here. These results were published in 2012. [14]

A second set of measurements was obtained in the field to determine the effect of season of the year on the acoustic attenuation in seagrass meadows. The results are shown in Fig. 5. During the winter season, seagrass goes dormant and photosynthetic activity is at a minimum or ceases entirely. There is no added attenuation due to the presence of seagrass at this time ofyear, as the measured attenuation was the same as that over a bare substrate. In the summer season, there is significant difference between propagation over bare substrate and propagation through seagrass. These measurements imply that mine detection in seagrass meadows would be better during the winter months, or otherwise when the seagrass is dormant.

Acoustics of Methane Hydrates: An article [22] was published this year on work completed in the previous FY. The paper shows that the ebullition rate of bubbles from methane seeps can be detected and quantified acoustically. There is no absolute standard

for accuracy in this case, but the acoustic method exhibited significantly less measurement uncertainty than the competing methods (optical, and gas trap).

Objective 2 —SW06 Analysis and CSS Development:

SW06 Analysis: Jason D. Sagers, a Graduate Fellowship Special Awards in Ocean Acoustics recipient, studied the effect of internal waves on shallow water acoustic fluctuations using data collected from SW06. Jason completed his PhD dissertation and graduated in August 2012. This PI served as co-supervisor along with David Knobles. The goal of the dissertation was to answer the following question: Given the data from the coincident acoustic and oceanographic measurements in SW06, to what degree can acoustic intensity fluctuations be predicted in the presence of internal waves? There is a large amount of SW06 acoustic and oceanographic data analysis in the dissertation and some examples are shown here. In Fig. 6, measured and modeled depth-averaged acoustic intensity $I_z(t)$ received on a vertical line array downrange from the source are compared for 31 internal wave events. The qualitative agreement between the measured and modeled acoustic data is good at both long- and short-temporal scales. The general level of agreement between the measured and modeled acoustic intensity $I_z(t)$ represents one of the major accomplishments of the work. Namely, the novel process Sagers used for creating the oceanographic model (evolutionary propagated thermistor string, or EPTS), captures the physics that drive the details of the acoustic fluctuations. This suggests that deterministic modeling of the acoustic fluctuations caused by internal waves is possible, to some degree, provided that sufficient information is known about the range- and time-dependent water column sound speed profile.

In addition to the deterministic modeling, Sagers also conducted analysis of the statistics of the acoustic intensity fluctuations and compared them to the statistics of the model predictions. An example is shown in Fig. 7, which provides evidence that the combination of the oceanographic and acoustic model is able to reproduce the received level statistics for time scales on the order of internal wave events. The widths of the distributions in Figs. 7(a) and 7(b) for energetic internal wave events are considerably larger than for the much less energetic internal wave event shown in Fig. 7(c) and reflects the fact that internal waves can cause dramatic fluctuations in the received acoustic signal.

CSS Development: In preparation for future sea tests, we are building a towable and ocean bottom deployable version of the combustive sound source (CSS). Firing CSS in open water is becoming more difficult due to environmental regulations limiting sound levels in the water, even for this source, which is intended to replace SUS. The CSS towbody is nearing completion and a tow test is planned for Fall 2012 at the Naval facility at Lake Glendora, Indiana. A picture of the CSS towbody is shown in Fig. 8, which contains the electrolytic gas generator, the ignition system, the CSS combustion chamber, and the electronics package required to control the system. An electromechanical cable provides electrical and power and control signals. No energetic materials are stored on deck, as the combustible gas mixture is generated *in situ*.

Objective 3—Future Sea Test Planning:

The PI serves as co-chief scientist (with David Knobles) for the Sediment Characterization Experiment, an upcoming ONR-sponsored shallow water sea test to be fielded in 2014–15. This activity includes attending and participation in several workshops held at ASA meetings and stand-alone workshops in January in Arlington.

Objective 4—3-D Inversion for Sound Speed and Temperature:

Graduate student Christopher M. Bender is nearing completion of his MS Thesis entitled *Three-Dimensional Geoacoustic Perturbative Inverse Technique for the Shallow Ocean Water Column*. In addition to describing the 3D inversion scheme and its optimization, Bender's thesis will address the following: the effect of domain and bathymetry discretization, and the effect of source and receiver density. Typical results from an inversion run on simulated acoustic data are shown in Fig. 9. In this case, depth averaged sound speed inversion error was less than 0.5 m/s throughout the 4500 square kilometer, 49 inversion cell area. The effect of source/receiver density and environmental discretization resolution is shown in Fig. 10. As expected, increasing the number of acoustic paths, by increasing the number of sources and receivers reduces sound speed inversion error, but an unexpected result is that the coarse environmental sampling yields a more accurate inversion.

Objective 5—Bubble discriminating sonar proof-of-concept:

Post-doctoral associate Kevin M. Lee developed a laboratory-scale proof-of-concept demonstration sonar system which can automatically discriminate between solid object targets and bubbles. The basic functionality of the system and example signals are described in Fig. 11. An additional apparatus schematic and an example sonar image are shown in Fig. 12. The details of the system, its operation, and an explanation of the results are given in the figure captions, but in short, the figures demonstrate that this proof-of-concept system can automatically discriminate between echoes returning from bubble clouds and solid elastic targets.

Finally, a full listing of all grant-related publication activities is shown in the Fiscal Year Publications section below the References section.

IMPACT/APPLICATIONS

Sandy sediments: The Biot-based description of sound propagation within sandy marine sediments has support in the ocean acoustics and related research communities, but we are also coming to the conclusion that it not fully adequate. Our laboratory results reported last year [13] showed that the Biot-Stoll model [17, 21] correctly predicts the porosity dependency of the high frequency sound speed in water-saturated sand. Low frequency (53–2000 Hz) attenuation data [10] from SW06 are also well described by Biot-Stoll and clearly follow the low frequency limiting slope of frequency squared. The data obtained this year show that neither Biot-Stoll [17, 21] nor the BICSQS model [20] can simultaneously predict both sound speed and attenuation for a single set of model input parameters over a wide frequency range (10–900 kHz). Despite many years of

study, we still do not fully understand sound propagation in idealized laboratory water-saturated granular sediments, much less in real ocean-bottom sediments.

Sound propagation in seagrass: Both lab and field studies revealed that the acoustic attenuation of sound propagating in seagrass meadows exhibits both diurnal and seasonal dependencies. During winter months, seagrass goes dormant, photosynthesis diminishes, and acoustic attenuation is also at a minimum. Winter is therefore the optimum time to conduct mine hunting in seagrass meadows. Conversely, during summer months, the plants are photosynthetically active, attenuation is the highest, and mine hunting would likely be less successful than in the winter. On the diurnal time scale, the attenuation varies from day to night, but the variation is species dependent. In general, attenuation is highest in the morning and lowest at night, but some species show less dependence on the diurnal cycle than others. Optimizing mine hunting on the diurnal cycle will require this specific knowledge for each species of interest.

Intensity fluctuations in shallow water due to internal waves: The acoustic intensity fluctuations that are observed in shallow water sound propagation in the presence of internal waves can be predicted if sufficient knowledge of the oceanographic conditions is available. This result was achieved with the sampling density of the SW06 field experiment. It remains to be determined how much environmental information is sufficient for a particular desired level of predictive accuracy.

CSS as an alternative to underway SUS deployment: The towable version of CSS is nearly ready for open water testing. It will be a self-contained tow body, producing its own gaseous fuel and oxidizer on demand *in situ*, and will require only mechanical and electrical connections to the tow vessel.

3D inversion for sound speed and temperature: Accurate, large-scale 3D sound speed inversion was demonstrated using simulated acoustic data in the New Jersey Hudson Canyon shelf environment. Increasing the source and receiver density increases the accuracy (not surprisingly) but increasing the resolution of the environmental grid does not increase inversion accuracy.

Bubble discriminating sonar: We successfully demonstrated a proof-of-concept laboratory bubble discriminating sonar system. The system exploits nonlinearities associated only with bubbles and uses those features to automatically detect echoes from bubbles. Once detected echoes from the bubbles were marked on the sonar display to positively identify clutter due to bubbles (or swim bladders) and thereby discriminate between clutter and solid targets.

TRANSITIONS

This PI received the final funding increment in the reporting fiscal year from the Naval Oceanographic Office for further development of the combustive sound source (CSS) as a replacement for explosives in ocean surveys. This was the second and final year of a DURIP award to develop the CSS for use in ocean acoustics experiments. This PI

continued a project originally started in 2009, funded by Shell Oil, to use bubbles to reduce the radiated noise from offshore drilling operations. Much of this PI's experience with bubbles was due to a project previously funded by ONR and also due to the current grant. This PI also leveraged previous OA funding to receive a grant on the Basic Research Challenge Fish Acoustics program, which continued in this FY. Finally, successful results with the bubble discriminating sonar led to discussions with ONR program officers about possible future transitions of this technology.

RELATED PROJECTS

SAX99: Sediment Acoustics Experiment 1999
From the project web page: SAX99 addresses high-frequency sound penetration into, propagation within, and scattering from the shallow-water seafloor at a basic research (6.1) level.
http://www.apl.washington.edu/programs/SAX99/Program/prog.html

SAX04: Sediment Acoustics Experiment 2004
From the project web page: The overall objective of SAX04 is to better understand the acoustic detection at low grazing angles of objects, such as mines, buried in sandy marine sediments. One component of the SAX04 work is designed to collect data and gain a greater understanding of high-frequency sound penetration into, propagation within, and scattering from the shallow water seafloor at a basic research level. A second component is designed to provide data directly on acoustic detections of buried mine-like objects at low grazing angles.
http://www.apl.washington.edu/projects/SAX04/summary.html

Other ARL:UT sediment researchers: Marcia Isakson and Nicholas Chotiros both conduct research on sound propagation in marine sediments. Many ONR PIs conduct research on modeling of sound propagation in shallow water waveguides.

REFERENCES

[1]   P.S. Wilson, R.A. Roy, and W.M. Carey, "An improved water-filled impedance tube," *J. Acoust. Soc. Am.* **113**, pp. 3245–3252 (2003).
[2]   P.S. Wilson, R.A. Roy, and W.M. Carey, "Phase speed and attenuation in bubbly liquids inferred from impedance measurements near the individual bubble resonance frequency," *J. Acoust. Soc. Am.* **117**, pp. 1895–1910 (2005).
[3]   T.F. Argo IV and P.S. Wilson, "Low-frequency laboratory measurements of sound speed in water-saturated granular sediments (A)," *J. Acoust. Soc. Am.* **120**, pp. 3098 (2006).
[4]   P.S. Wilson, A.H. Reed, J.C. Wilbur, and R.A. Roy, "Evidence of dispersion in an artificial water-saturated sand sediment," *J. Acoust. Soc. Am.* **121**, pp. 824–832 (2007).
[5]   P.S. Wilson, A.H. Reed, W.T. Wood, and R.A. Roy, "Low frequency sound speed measurements paired with computed x-ray tomography imaging in gas-bearing reconstituted natural sediments," in *Proceedings of the 2nd International*

Conference and Exhibition on Underwater Acoustics Measurements: Technologies and Results, J. S. Papadakis and L. Bjørnø, Eds. Heraklion, Greece, 2007, pp. 21–29, ISBN 978-960-88702-5-3.

[6]   P.S. Wilson, A.H. Reed, W.T. Wood, and R.A. Roy, "The low-frequency sound speed of fluid-like gas-bearing sediments," *J. Acoust. Soc. Am.* **123**, pp. EL99–EL104 (2008).

[7]   P.S. Wilson and K.H. Dunton, "Seagrass acoustics: Results of an experimental laboratory investigation," in *Proceedings of the 2nd International Conference and Exhibition on Underwater Acoustics Measurements: Technologies and Results*, J. S. Papadakis and L. Bjørnø, Eds. Heraklion, Greece, 2007, pp. 383-390, ISBN 978-960-88702-5-3.

[8]   P.S. Wilson and K.H. Dunton, "Laboratory investigation of the acoustic response of seagrass tissue in the frequency band 0.5–2.5 kHz," *J. Acoust. Soc. Am.* **125**, pp. 1951–1959 (2009).

[9]   P.S. Wilson, "From bubbles to sediments to seagrass: Wood's equation in underwater acoustics," in *International Conference on Detection and Classification of Underwater Targets*, vol. 29, Pt. 6. Hertfordshire, UK: Institute of Acoustics, 2007, pp. 138-146, ISBN 1-901656-88-8 (http://asa.aip.org/awards.html).

[10]   D.P. Knobles, P.S. Wilson, S. Cho, and J.A. Goff, "Seabed acoustics of a sand ridge on the New Jersey continental shelf," *J. Acoust. Soc. Am.* **124**, pp. EL151–EL156 (2008).

[11]   J.A. TenCate, T.G. Muir, A. Caiti, A. Kristensen, J.F. Manning, J.A. Shooter, R.A. Koch, and E. Michelozzi, "Beamforming on seismic interface waves with an array of geophones on the shallow sea floor," *IEEE Journal of Oceanic Engineering,* **20**, pp. 300–310 (1995).

[12]   E. Smith, P.S. Wilson, F.W. Bacon, J.F. Manning, J.A. Behrens, and T.G. Muir, "Measurement and localization of interface wave reflections from a buried target," *J. Acoust. Soc. Am.* **103**, pp. 2333–2343 (1998).

[13]   T.F. Argo IV, M.D. Guild, P.S. Wilson, M. Schroter, C. Radin, and H.L. Swinney, "Sound speed and attenuation in water-saturated glass beads as a function of frequency and porosity," *J. Acoust. Soc. Am.* **129**, pp. EL101–107 (2011).

[14]   C.J. Wilson, P.S. Wilson, and K.H. Dunton, "An acoustic investigation of seagrass photosynthesis," *Marine Biology* **159**, pp. 2311–2322 (2012).

[15]   K.M. Lee, K.T. Hinojosa, M.S. Wochner, T.F. Argo, P.S. Wilson, and R.S. Mercier, "Sound propagation in water containing large tethered spherical encapsulated gas bubbles with resonance frequencies in the 50 Hz to 100 Hz range," *J. Acoust. Soc. Am.* **130**, pp. 3325–3332 (2011).

[16]   D.P. Knobles, J.A. Goff, R.A. Koch, S.M. Joshi, P.S. Wilson, and J.A. Shooter, "Modeling broadband acoustic propagation in an uncertain inhomogeneous shallow water ocean waveguide," *IEEE Journal of Oceanic Engineering* **35**, pp. 732–742 (2010).

[17]   R.D. Stoll and T.K. Kan, "Reflection of acoustic waves at a water–sediment interface," *J. Acoust. Soc. Am.* **70**, pp. 149–156 (1981).

[18] T.F. Argo IV, *Laboratory Measurements of Sound Speed and Attenuation of Water-Saturated Granular Sediments*, Ph.D. Dissertation, The University of Texas at Austin (2012).

[19] J.-X. Zhou, X.-Z. Zhang, and D. P. Knobles, "Low-frequency geoacoustic model for the effective properties of sandy seabottoms," *J. Acoust. Soc. Am.* **125**, pp. 2847–2866 (2009).

[20] N. P. Chotiros and M. J. Isakson, "High-frequency dispersion from viscous drag at the grain-grain contact in water-saturated sand, " *J. Acoust. Soc. Am.* **124**, pp. 1–6 (2008).

[21] R. D. Stoll, *Sediment Acoustics*, Springer-Verlag, New York (1989).

[22] C.A. Greene and P.S. Wilson, "Laboratory investigation of a passive acoustic method for measurement of underwater gas seep ebullition," *J. Acoust. Soc. Am.* **131**, pp. EL61-EL66 (2011).

GRANT-RELATED PUBLICATIONS THIS FISCAL YEAR

Archival Journal Papers

[1] K.M. Lee, K.T. Hinojosa, M.S. Wochner, T.F. Argo, P.S. Wilson, and R.S. Mercier, "Sound propagation in water containing large tethered spherical encapsulated gas bubbles with resonance frequencies in the 50 Hz to 100 Hz range," *J. Acoust. Soc. Am.* **130**, pp. 3325–3332 (2011).

[2] C.A. Greene and P.S. Wilson, "Laboratory investigation of a passive acoustic method for measurement of underwater gas seep ebullition," *J. Acoust. Soc. Am.* **131**, pp. EL61–EL66 (2011).

[3] C.J. Wilson, P.S. Wilson, and K.H. Dunton, "An acoustic investigation of seagrass photosynthesis," *Marine Biology* **159**, pp. 2311–2322 (2012).

Conference Papers and Proceedings

[1] T.F. Argo IV and P.S. Wilson, "Implications of the presence of shell hash on the speed and attenuation of sound in water-saturated granular sediments," *J. Acoust. Soc. Am.* **130**, pp. 2381–2381 (2011).

[2] J.I. Arvelo, J. Dietz, A.R. McNeese, J.D. Sagers, and P.S. Wilson, "Initial assessment of combustive sound source arrays as airgun alternatives for Arctic under-ice seismic exploration," *J. Acoust. Soc. Am.* **130**, pp. 2413–2413 (2011).

[3] C.M. Bender, M.S. Ballard, and P.S. Wilson, "Estimates of the water column sound-speed field in three dimensions using a linearized perturbative technique," *J. Acoust. Soc. Am.* **130**, pp. 2455–2455 (2011).

[4] J. Giard, G.R. Potty, J.H. Miller, J.M. Greene, A.R. McNeese, and P.S. Wilson, "Estimation of shear speed using interface wave dispersion," *J. Acoust. Soc. Am.* **130**, pp. 2392–2392 (2011).

[5] T.A. Hay, Y.A. Ilinskii, E.A. Zabolotskaya, P.S. Wilson, and M.F. Hamilton, "A model for noise radiated by submerged piles and towers in littoral environments," *J. Acoust. Soc. Am.* **130**, pp. 2558–2558 (2011).

[6] J. Arvelo, J. Dietz, A.R. McNeese, J.D. Sagers, and P.S. Wilson, "Initial assessment of combustive sound source arrays as airgun alternatives for Arctic

under-ice seismic exploration," *Proceedings of Meetings on Acoustics* **14**, pp. 070004–10 (2012).

[7]   C.M. Bender, M.S. Ballard, and P.S. Wilson, "Range and cross-range resolution from a three-dimensional linearized perturbative inversion scheme," *J. Acoust. Soc. Am.* **132**, pp. 2093–2093 (2012).

[8]   C.M. Bender, M.S. Ballard, and P.S. Wilson, "Estimates of the water column sound-speed field in three dimensions using a linearized perturbative technique," *Proceedings of Meetings on Acoustics* **14**, pp. 070006–12 (2012).

[9]   K.M. Lee, K.T. Hinojosa, M.S. Wochner, T.F. Argo Iv, and P.S. Wilson, "Mitigation of low-frequency underwater sound using large encapsulated bubbles and freely-rising bubble clouds," *Proceedings of Meetings on Acoustics* **12**, pp. 070006–15 (2012).

[10]   K.M. Lee, A.R. McNeese, L.M. Tseng, M.S. Wochner, and P.S. Wilson, "Measurements of resonance frequencies and damping of large encapsulated bubbles in a closed, water-filled tank," *J. Acoust. Soc. Am.* **132**, pp. 2039–2039 (2012).

[11]   K.M. Lee, A.R. McNeese, M.S. Wochner, and P.S. Wilson, "Reduction of underwater sound from continuous and impulsive noise sources using tethered encapsulated bubbles," *J. Acoust. Soc. Am.* **132**, pp. 2062–2062 (2012).

[12]   K.M. Lee, M.S. Wochner, and P.S. Wilson, "Mitigation of underwater radiated noise from a vibrating work barge using a stand-off curtain of large tethered encapsulated bubbles," *J. Acoust. Soc. Am.* **132**, pp. 2056–2056 (2012).

[13]   K.M. Lee, M.S. Wochner, and P.S. Wilson, "Mitigation of low-frequency underwater noise generated by rotating machinery on a mobile work barge using large tethered encapsulated bubbles," *J. Acoust. Soc. Am.* **131**, pp. 3507–3507 (2012).

[14]   A.R. McNeese, T.G. Muir, and P.S. Wilson, "Investigation of a tunable combustive sound source," *J. Acoust. Soc. Am.* **132**, pp. 2056–2056 (2012).

[15]   G.R. Potty, J.H. Miller, J. Giard, A.R. McNeese, P.S. Wilson, and Y.-M. Jiang, "Shear wave speed inversions using scholte wave dispersion," *J. Acoust. Soc. Am.* **131**, pp. 3241–3241 (2012).

[16]   M.S. Wochner, K.M. Lee, and P.S. Wilson, "Attenuating underwater pile driving noise at a remote receiving location using an encapsulated bubble curtain," *J. Acoust. Soc. Am.* **131**, pp. 3356–3356 (2012).

HONORS/AWARDS/PRIZES

National Geographic covered our work on the acoustics of bubbly liquids and their use for underwater noise abatement in the September 2012 print issue and online:

http://news.nationalgeographic.com/news/energy/2012/02/120207-bubble-curtains-to-protect-whales/

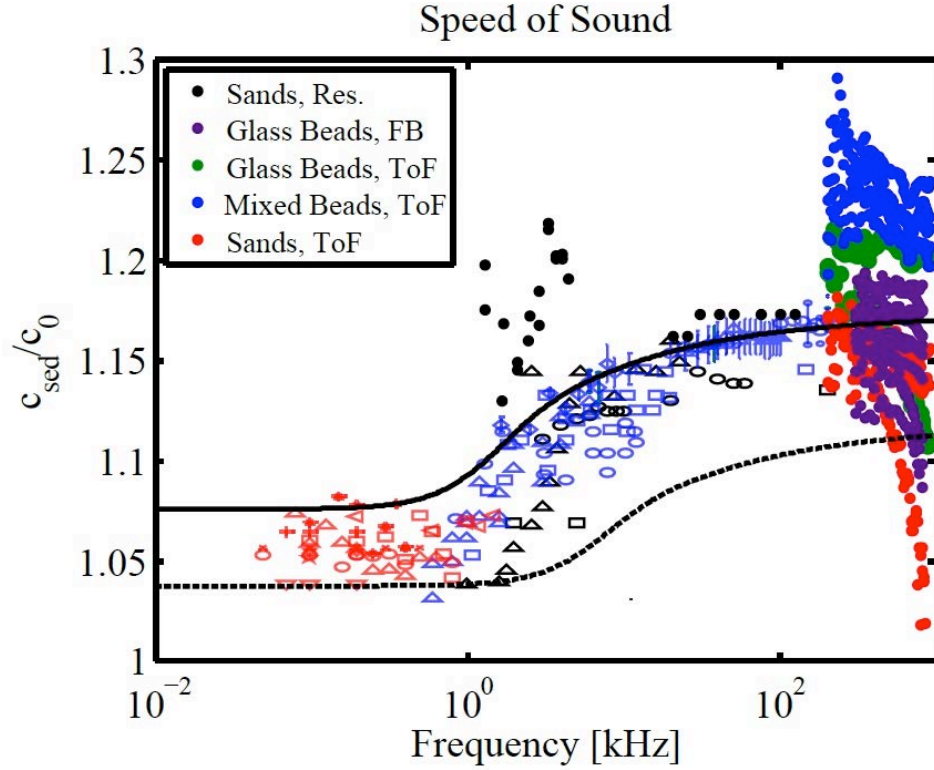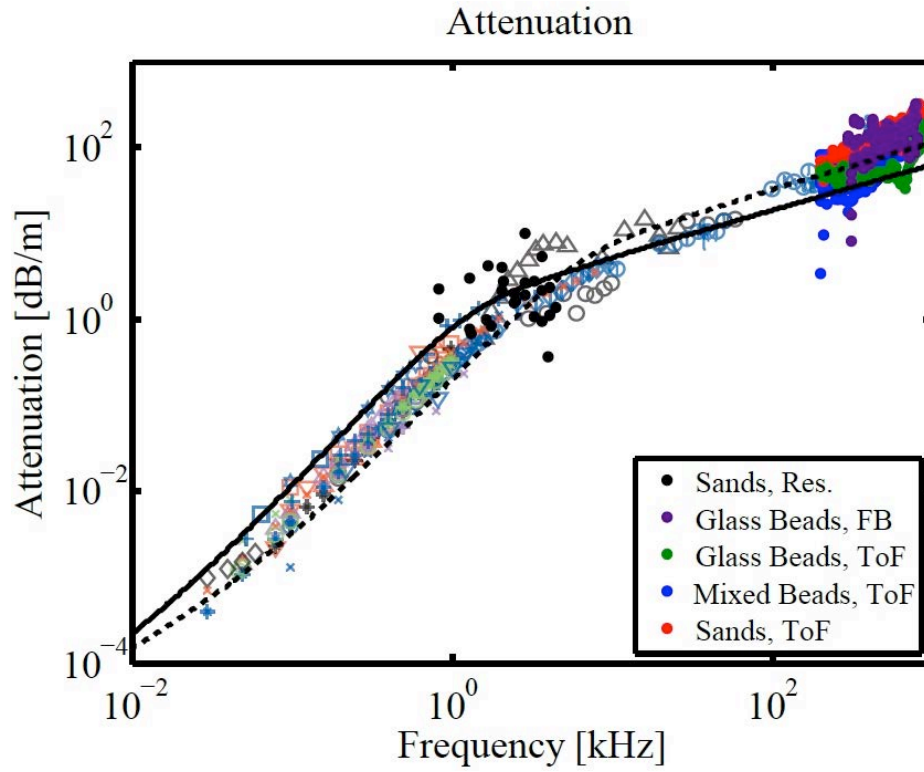# FIGURES

Speed of Sound

Fig. 1. All the speed of sound measurements from Argo's dissertation [18] are shown (filled data points) and are compared to the measurements reported in [19] (unfilled data points), which are all *in situ* measurements of sound propagation in sandy sediments. The Biot-Stoll model curves provided from [19] are plotted for the range of material parameters from the SAX99 (upper solid line) and SAX04 (lower dashed line) experiments. The low frequency resonator measurements (solid black circles) from Chapter 3 of [18] have a faster speed of sound than the literature *in situ* data and the time-of-flight measurements from Chapter 3 of [18] agree well with the model predictions for the SAX99 experiment. Sands with similar properties to the SAX99 sediment measured using the time-of-flight technique from Chapter 5 of [18] (solid red circles) show agreement in sound speed at 200 kHz and exhibit negative dispersion at higher frequencies. See [18] for a full description of the data. Much of the data is not expected to agree with the in situ measurements and SAX-parameter models.

Fig. 2. A plot of all attenuation measurements from Argo's dissertation [18] are shown (filled data points) and are compared to the measurements reported in [19] (unfilled data points), which are all *in situ* measurements of sound propagation in sandy sediments.. The Biot-Stoll model curves provided from [19] are plotted for the range of material parameters from the SAX99 (solid line) and SAX04 (dashed line) experiments. The attenuation measurements (solid black circles) from the low-frequency resonator apparatus in Chapter 3 of [18] are in general agreement with the model predictions. Measurements on sands similar to those in the SAX99 experiments using the time-of-flight apparatus from Chapter 5 of [18] shown in red agree with the Biot-Stoll model plotted for the material properties from the SAX04 experiment around 200 kHz. As frequency is increased, the attenuation accelerates in growth and is no longer predicted by the model.
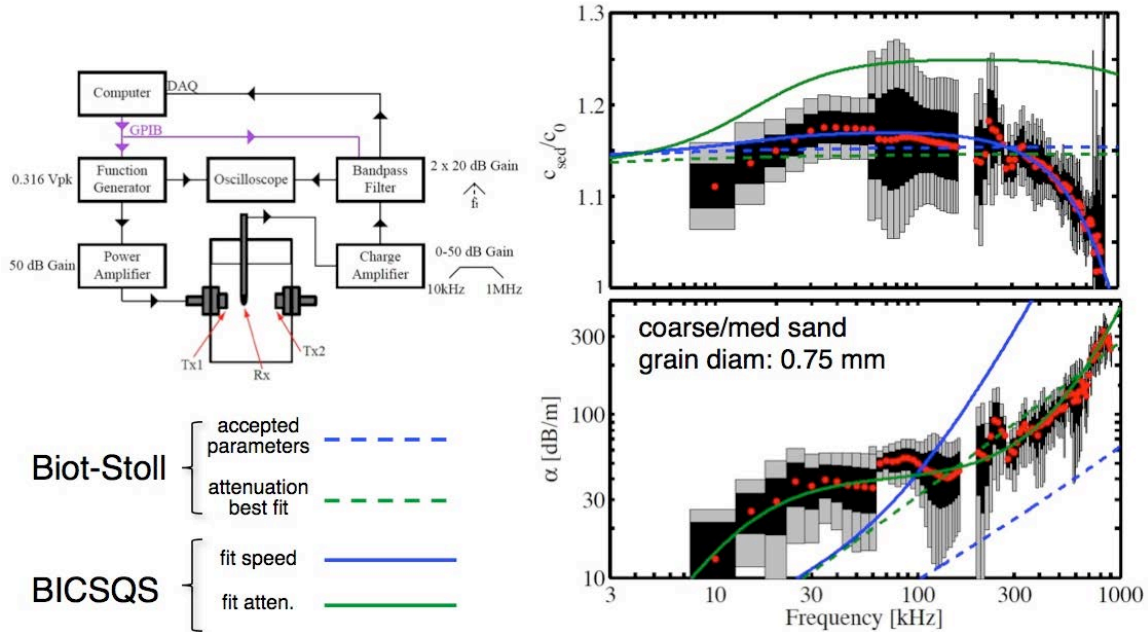
Fig. 3. An overview of sound speed (upper right) and attenuation measurements (lower right), are shown as a function of frequency in course/med water-saturated sand. The data were obtained with the apparatus shown on the upper left using three pairs of transducers, to span the frequency range. Red dots represent the mean value at each frequency, the black bars represent one standard deviation and the gray bars represent the 95% confidence interval of the data at each frequency. Model curves are also shown (see the legend at the lower left). The BICSQS model can be fit to *either* the sound speed *or* the attenuation (using *different* input parameters), and is in all cases a better fit than the Biot-Stoll model. *Neither* model can be made to fit *both* sound speed and attenuation for the *same* set of input parameters.
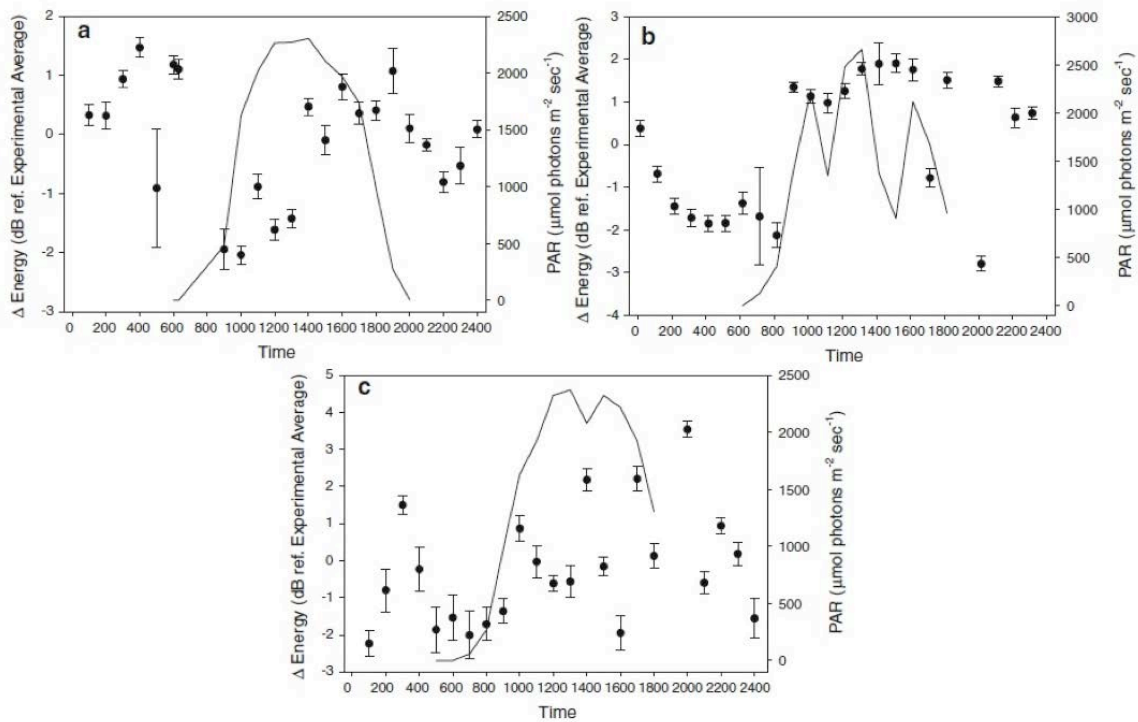
Fig. 4. Change in the received acoustic energy at 100 kHz propagating through reconstituted seagrass meadows, and available photosynthetically active radiation (PAR) over a 24-h period with a) *S. filiforme*, b) *H. wrightii* and c) *T. testudinum*. Data points represent the mean acoustic intensity relative to the 24-h experimental average, and the error bars represent standard deviation (n = 10). The lines denote the trend in mean hourly PAR measurements.
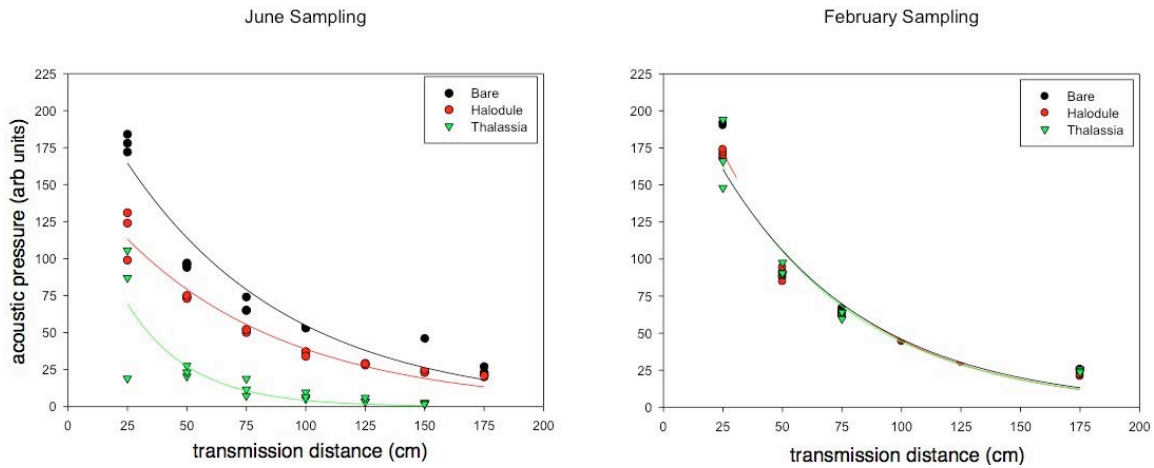

Fig. 5. Received acoustic pressure at 100 kHz for sound propagation through natural meadows of *H. wrightii*, *T. testudinum,* and bare sediment, as a function of distance from the source for June (active) and February (inactive) photosynthetic seasons of the year. In the left-hand plot, for June, when photosynthesis is active, the acoustic received level is reduced for *Halodule* and further reduced for *Thalassisa*, relative to the bare substrate. In the right-hand plot, for February, when the plants are dormant and there is no photosynthetic activity, there is no difference in received acoustic level due to the presence or species of seagrass. This implies that mine detection in seagrass beds might be easier during the dormant season.
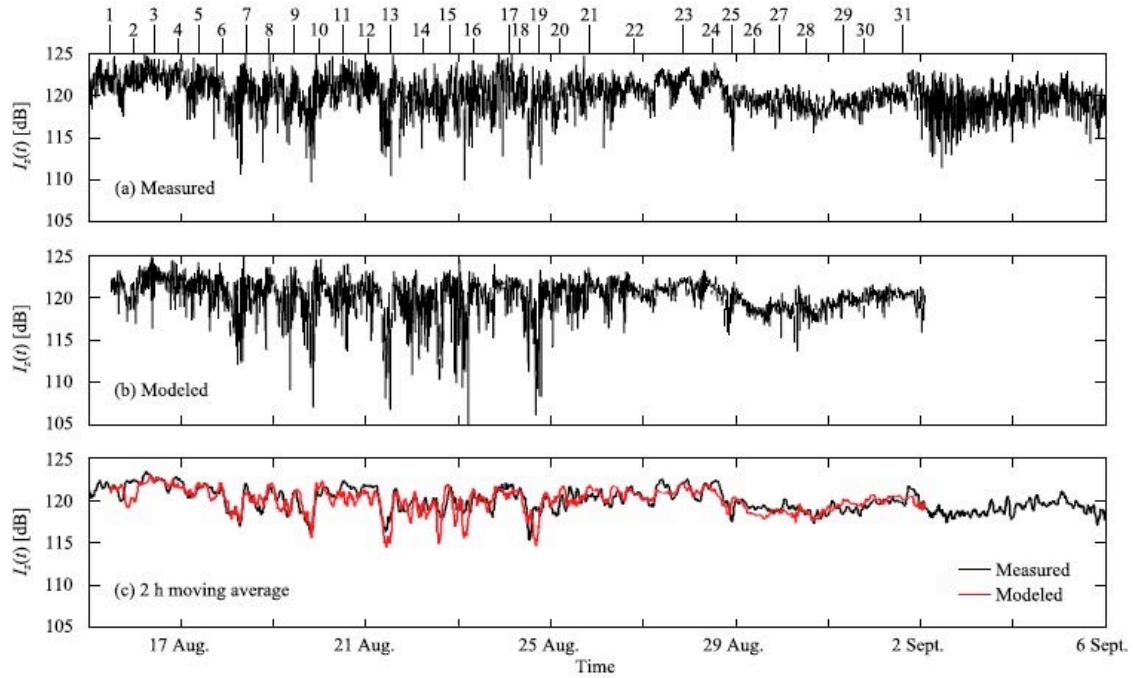
Fig. 6. Comparison between (a) measured and (b) modeled depth-averaged acoustic intensity $I_z(t)$ with IW event times labeled above the figure. (c) shows measured and modeled $I_z(t)$ after a 2-h moving average filter.
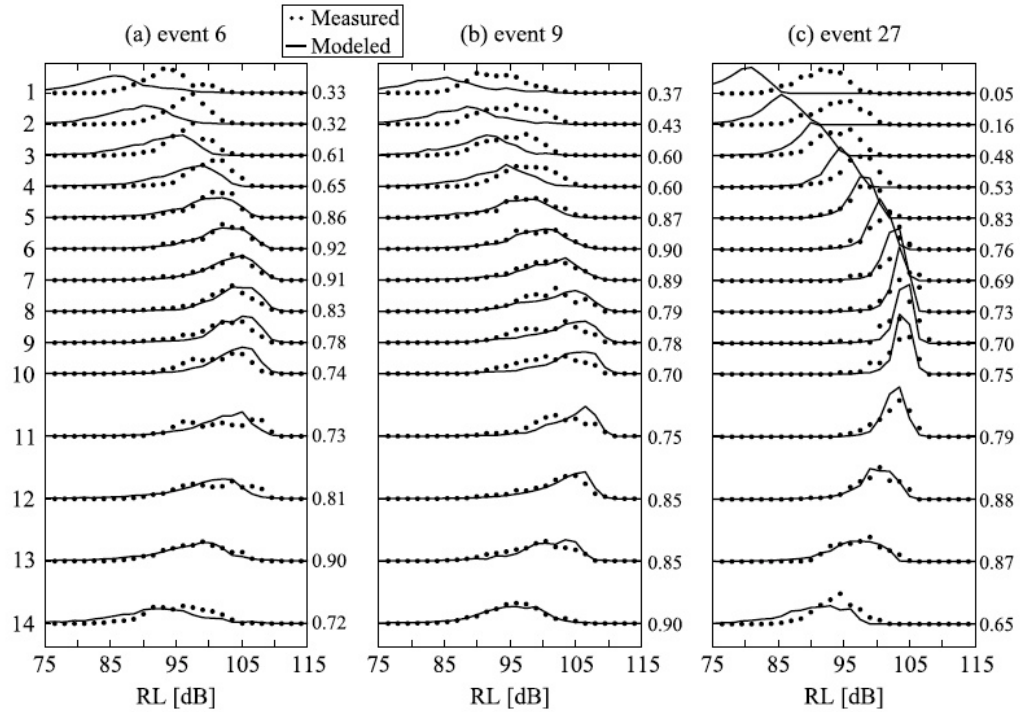

Fig. 7. Received-level distributions for three internal wave events during SW06. The distributions are spaced vertically according to the depth of the hydrophone in the water column and the overlap values comparing each of the measured and modeled distributions are shown to the right of each distribution.
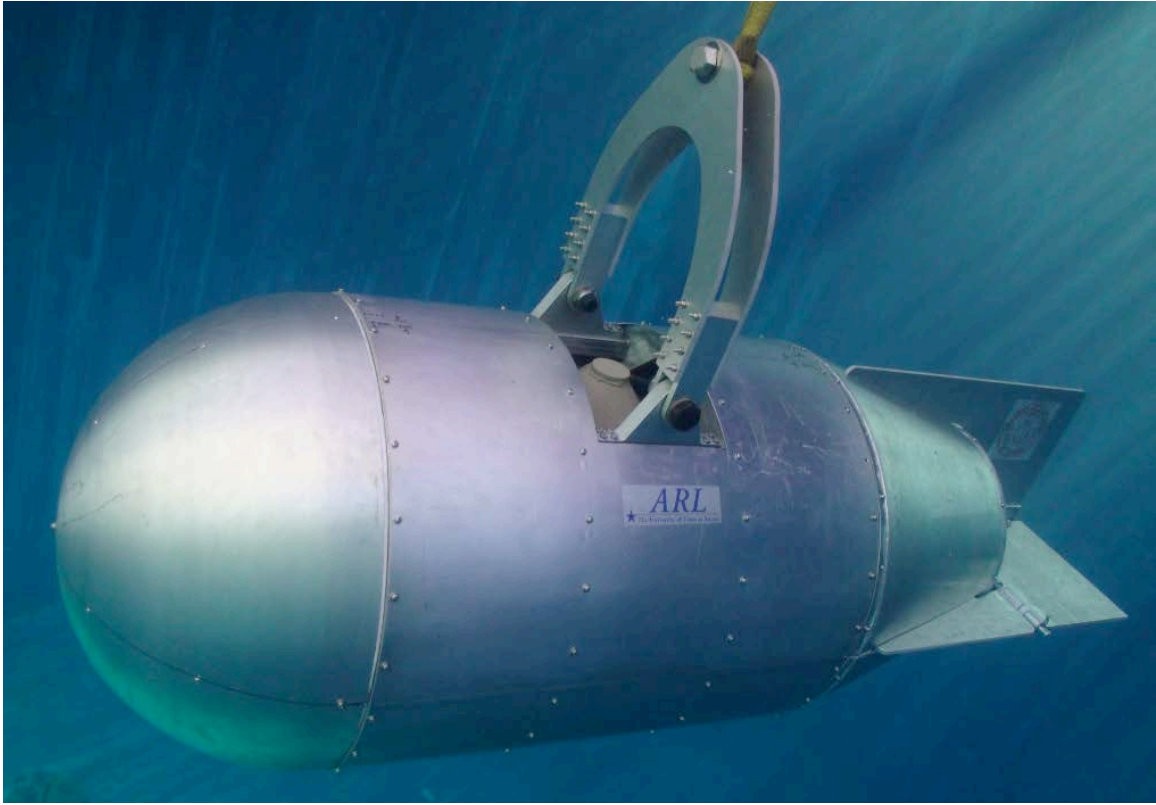
Fig. 8. A photograph of the CSS contained within its towbody is shown inside the ARL test tank.
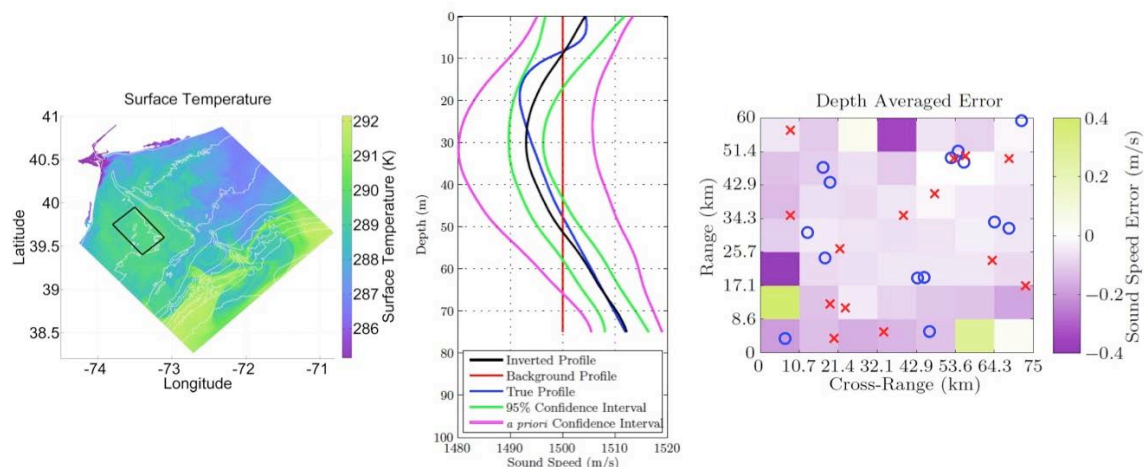
Fig. 9. Simulated ocean temperature field near the SW06 site (left). Only surface temperatures are shown (with the color scale) but full water column temperatures are known. The black rectangle represents the area over which the inversion scheme was run. In the middle, a set of representative sound speed profiles from one inversion grid sub-section is shown. On the right, depth-averaged inversion sound speed errors are shown using the color scale. Good agreement between true and inverted sound speeds was obtained. The blue circles show the locations of the sources and the red crosses show the locations of the receivers.
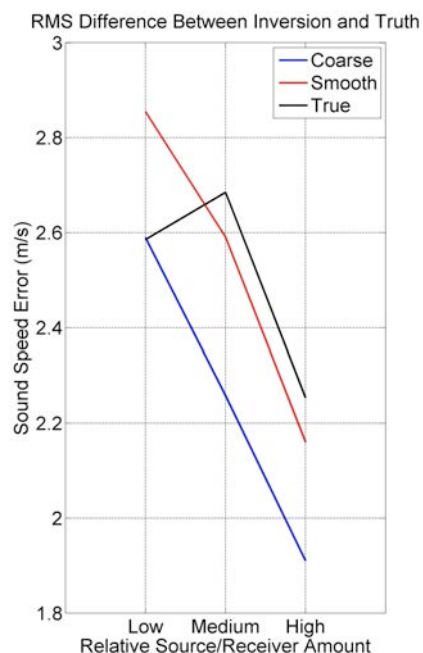

Fig. 10. The effect of source/receiver density (horizontal axis) and environmental resolution (blue, red and black curves) on global mean inversion sound speed error (vertical axis) is shown. As expected, increasing the number of acoustic paths (by increasing the number of sources and receivers) reduces error, but an unexpected result is that the coarse environmental sampling yields the most accurate inversion.
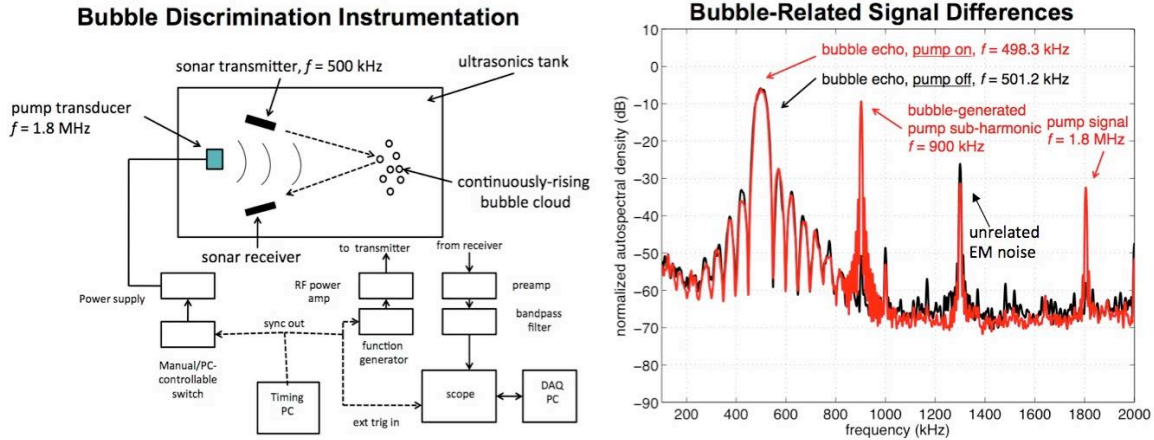
Fig. 11. The left side shows a schematic diagram of the bubble-discriminating proof-of-concept sonar system. The system is contained within a laboratory desk-top tank. The imaging "sonar" consists of a pair of send/receive 500 kHz transducers. There is also a 1.8 MHz "pump" transducer which induces Doppler shift and a pump signal subharmonic at 900 kHz in echoes from the bubble cloud target. Example signals generated by this system are shown on the right. The black curve is the sonar bubble cloud echo signal with the pump *inactive* showing a strong return at 498.3 kHz. The red curve is the sonar echo signal with the pump *active*. The bubble echo has shifted to 501.2 kHz due to a Doppler shift caused by the pump signal inducing motion of the bubble cloud target. Not shown is the absence of any Doppler shift on a solid elastic target in the presence of the pump signal. Also visible in the red signal are the primary (1.8 MHz) and subharmomnic (900 kHz) lines due to the pump signal. The submarmoic is due to nonlinear motion of the bubbles in the target region induced by the pump signal. Notice the 900 kHz subharmonic line is absent in the black curve. Not shown is the absence of a subharmonic signal in a target return from a solid object. Hence, only bubbles will exhibit both induced Doppler and pump subharmonic signals, and solid elastic objects will not.
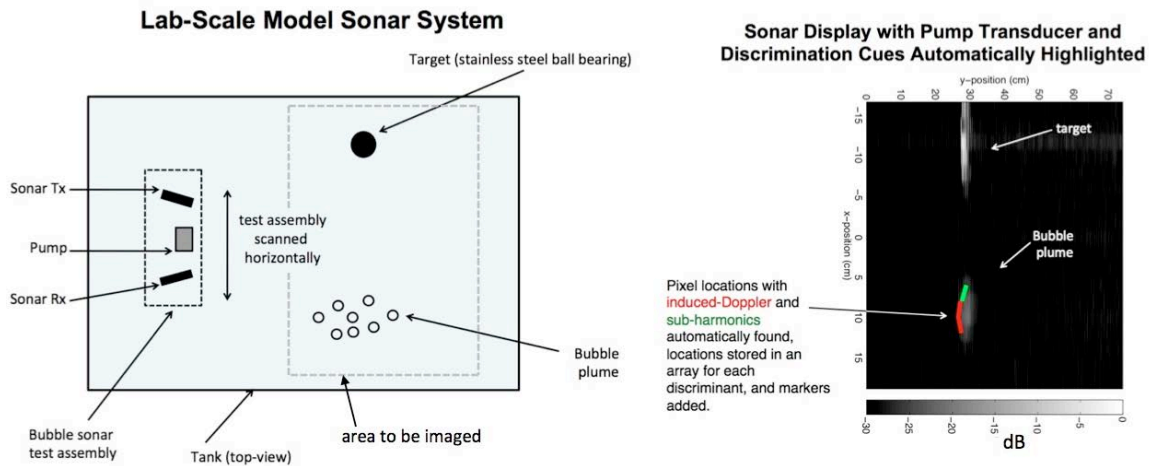

Fig. 12. Whereas Fig. 11 described the basis for processing a single echo, this figure shows how a sonar image is created. A schematic diagram of the bubble-discriminating system (left) now includes a scanning apparatus to physically scan the system across an area. A stainless steel spherical target is present along with a bubble plume. The gray dashed rectangle within the tank indicates the imaging region of the sonar. Echoes from the target region are collected at several positions along the scan axis and an image is built up from processed echoes. An example image is shown (right). Black regions indicate no echo and hence no target present. Lighter colored regions within the image represent echoes from targets. Each pixel of the image was also processed automatically to detect the presence of an induced Doppler shift and the presence of a subharmonic. If the induced Doppler shift was present that pixel was noted and a red line was automatically drawn to connect those pixels. Three pixels were found with induced Doppler, hence there was a two-segment red line automatically added to the image at the location of those pixels. Similarly, two pixels were automatically found to contain subharmonics, and hence a single-segment green line was added. The green and red markers clearly indicate the presence of the bubble cloud, and the echoes from the steel target carry no markers. Hence the system has automatically discriminated between the bubbles and the target.